Nanoscale

ARTICLE

SERS Nanosensors for *In Vivo* Detection of Nucleic Acid Targets in a Large Animal Model

Received 00th January 20xx,
Accepted 00th January 20xx

DOI: 10.1039/x0xx00000x

www.rsc.org/

H. N. Wang,[a,b]† J. K. Register,[a,b]† A. M. Fales,[a,b]† N. Gandra,[a,b] E. H. Cho,[c] A. Boico,[c] G. M. Palmer,[c] B. Klitzman,[c] and T. Vo-Dinh*[a,b,d]

Although nanotechnology has led to important advances in *in vitro* diagnostics, the development of nanosensors for *in vivo* detection still remains a great challenge. We have previously developed a promising type of SERS nanosensor based on an OFF-to-ON "inverse Molecular Sentinel" (iMS) detection scheme for *in vitro* nucleic acid detection. The iMS nanosensor involves using plasmonics-active nanostars, which have tunable absorption bands in the near infrared (NIR) region of the 'tissue optical window', rendering them as an efficient sensing platform for *in vivo* optical detection. Here, for the first time, we show the proof-of-principle of *in vivo* nucleic acid target detection using the SERS iMS nanosensors implanted in the skin of a large animal model (pig). *Ex vivo* measurements were also performed using human skin grafts to demonstrate the detection of SERS nanosensors through tissue. In this work, a new core-shell nanorattle probe having Raman reporters trapped between the core and shell was utilized as the internal standard system for self-calibration. The results of this study illustrate the the usefulness and translational potential of SERS nanosensors for future use in *in vivo* biosensing.

Introduction

Raman spectroscopy is an optical detection technique that provides characteristic molecular and vibrational spectral information from target analytes. This sensing modality provides specific spectral "fingerprints" exhibiting very sharp peaks that allow sensing multiple targets simultaneously- or "multiplexing". Furthermore, virtually any wavelength of laser excitation could be used in Raman spectroscopy, which is an important feature that provides the capability to perform measurements within the spectral range where tissue components absorb the least, thus offering the highest penetration depth for light into biological tissue, a great advantage for *in vivo* studies. This optical range, often referred to as the "tissue optical window" is defined by hemoglobin and melanin absorption below 650 nm and water absorption above 900 nm.

Plasmonics-active nanosystems have receiving increasing interest for *in vivo* imaging and sensing applications using Raman detection. The term "plasmonics" is derived from the word plasmon that refers to the quanta associated with longitudinal waves propagating in matter through the collective motion of large numbers of electrons. When an electromagnetic (EM) radiation (e.g., laser) irradiates the nanostructured metallic surface, the conduction electrons in metallic nanostructures are oscillating at the same frequency of the excitation light and produce a secondary EM field in addition to the incident field. These enhanced EM effects on nanoparticles, referred to as localized surface plasmons (LSP), become concentrated at points of high curvature and significantly increase the absorbed and scattered light near the metallic surface, which can interact with molecules on or near the nanoparticle surface. Noble metal nanoparticles resonantly absorb and scatter in the visible to near-infrared (NIR) region of the EM spectrum upon excitation of their LSPs, making them suitable platforms for plasmonic devices.

Surface plasmons significantly increase the Raman scattering by several orders of magnitude, a technique called surface-enhanced Raman scattering (SERS).[1,2] Our laboratory has developed and applied various SERS plasmonic platforms including nanoparticles, nanopost arrays, nanowires and nanochips.[3-5] Among the wide variety of types of nanostructures, gold nanoparticles have been the most widely studied for many reasons. Noble metal nanoparticles such as gold exhibit this resonant scattering inside the "tissue optical window", which is suitable for *in vivo* studies.[6] We have previously developed surfactant-free gold nanostars (AuNS) which have absorption bands that are tunable in the NIR region of the "tissue optical window".[7] Nanostars exhibit excellent plasmonic properties owing to their multiple sharp branches, each with a strongly enhanced EM field localized at its tip (i.e. "lightning rod" plasmonic effect), rendering them more suitable and efficient for *in vivo* applications and SERS detection.[7-10]

[a] *Departments of Biomedical Engineering, Duke University, Durham, NC 27708, USA*
E-mail: tuan.vodinh@duke.edu
[b] *Fitzpatrick Institute for Photonics, Duke University, Durham, NC 27708, USA*
[c] *Medical Center, Duke University, Durham, NC 27710, USA*
[d] *Departments of Chemistry, Duke University, Durham, NC 27708, USA*
† These authors contributed equally to this work.

There have been previous studies that involved SERS measurements in live animals. Souza et al.[11] described a system for measuring self-assembled Au-imidazole complexes, paving the way for translation of this technology into mice. Stuart et al.[12] reported *in vivo* detection of glucose using SERS with a system that utilized an optical window in a rat model. Qian et al.[13] used antibody-conjugated SERS nanoparticle tags that recognize tumor epidermal growth factor receptors (EGFR) biomarkers for *in vivo* tumor targeting and detection. The SERS technique has subsequently been developed for *in vivo* diagnostics,[14-17] imaging[18-21] and theranostics.[7,9,22-25] However, *in vivo* detection of nucleic acid targets in live animals using SERS still remains a great challenge and has not been reported. Cell-free nucleic acids (such as DNA, mRNA and microRNA) circulating in body fluids have received increasing interest due to their diagnostic applications.[26-31] They have been proven to be potential biomarkers for various diseases. The exact nature of cell-free circulating nucleic acids is still an area of increasing research and a topic of extensive scientific inquiry. An *in vivo* nucleic acid sensing system could provide a useful tool for potential continuous health status sensing, long-term disease monitoring and point-of-care applications.

We have recently developed a new plasmonics-based detection platform for nucleic acid targets using an "OFF-to-ON" SERS signal switch upon target identification and capture.[32-34] This novel turn-on detection scheme is referred to as the "inverse Molecular Sentinel" (iMS) nanosensor to distinguish it from our previously developed Molecular Sentinel (MS) nanoprobes with an "ON-to-OFF" signal switch.[35,36] The iMS nanosensor system is composed of three parts: (1) a stem-loop DNA probe labeled with a Raman reporter, which provides the source of the Raman signal, (2) a plasmonics-active nanostar and (3) an unlabeled DNA strand. As shown in Figure 1, the "stem-loop" DNA probe, having a Raman label at one end, is immobilized onto a nanostar via a metal-thiol bond. A single-stranded, unlabeled DNA, serving as a "placeholder" strand, keeps the Raman label away from the nanostar surface by binding to the stem-loop probe. Because the electromagnetic SERS enhancement decreases significantly with increasing distance from the metallic surface, a dye molecule must be located very close to the metallic surface in order to experience the enhanced local plasmon field. Thus, in this configuration (i.e. in the absence of a target), the nanosensor is "open" with low SERS intensity ('Off' status). Upon exposure to a target nucleic acid analyte, the placeholder strand acting as a target capture strand leaves the nanostar surface following a non-enzymatic strand-displacement process: the target first binds to the toehold region (i.e. an overhang region of the probe-placeholder conjugate) and begins displacing the DNA probe from the placeholder via branch migration, and finally releases the placeholder from the nanosensor system. This allows the stem-loop structure to "close" and moves the Raman label onto the plasmonics-active surface yielding a strong SERS signal ('On' status).

In this study, we present, to the best of our knowledge, for the first time *in vivo* transdermal NIR-SERS detection of nucleic acid targets in a large animal model (pig) using functional iMS nanosensors. SERS signal detection with power densities below the American National Standards Institute (ANSI) standard for maximum permissible exposure on the skin at 785 nm was also demonstrated *ex vivo* using human skin grafts. The results of this study demonstrate the clinically relevant translational potential of the SERS iMS nanosensor technique for *in vivo* biosensing.

Experimental section

Gold nanostar (AuNS) synthesis

Gold nanostars were synthesized using a seed-mediated method. Detailed synthesis and characterization of the nanostars has been presented elsewhere.[7] Briefly, in 10 ml 0.25 mM $HAuCl_4$ solution, 10 µl of 1N HCl and 100 µl of 12 nm citrate gold seeds were added followed by the simultaneous addition of 100 µl of $AgNO_3$ and 50 µl of 100 mM Ascorbic Acid under stirring (700 rpm). The reaction was performed under room temperature, and the process was completed in less than a minute. Afterwards, 0.02% final concentration of Tween 20 was added and the solution underwent centrifugation wash (3000 ×g 15 min) once, was resuspended to 0.1 nM in 0.02%

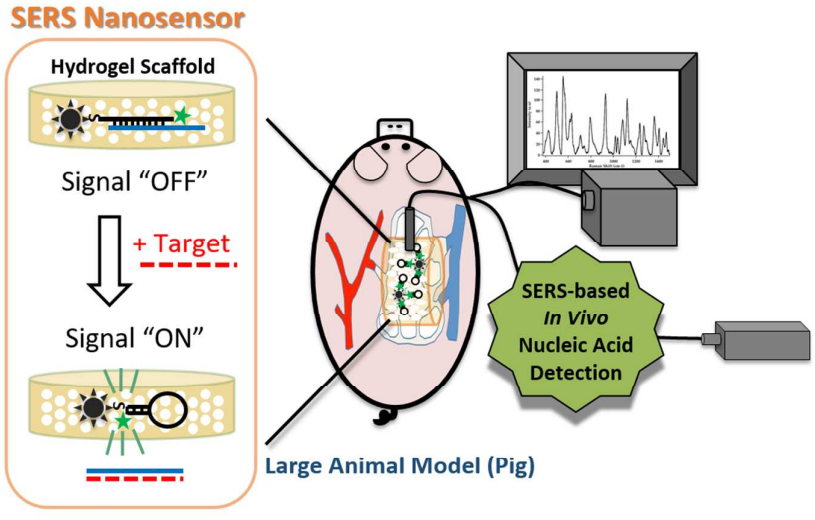

Fig. 1 *In vivo* nucleic acid detection scheme of the SERS iMS nanosensor in a large animal model (pig). A hydrogel matrix is used to protect the nanosensor from the complex biological environment.

Tween 20, and kept under 4 °C for long-term storage.

Silver-coated gold nanostar (AuNS@Ag) synthesis

The silver coating was performed as previously described.[10] A 1 mL aliquot of the washed AuNS solution was transferred into a 1.5 mL centrifuge tube. The sample was briefly vortexed after each subsequent chemical addition. Then 5µL of 0.1 M $AgNO_3$ and an equivalent volume of 0.1 M Ascorbic Acid (AA) were added to the solution. The reduction of silver by AA was initiated by the addition of 2µL NH_4OH, at which point the color of the solution began to darken. After about 5 minutes, the solution color had stabilized, indicating completion of the reaction. The silver coated AuNS were then labeled with dye by adding 1 µM final concentration of the desired dye (dissolved in EtOH) to the solution, allowing it to sit for 15 minutes, centrifuging at 2000 relative centrifugal force (rcf) for 10 minutes, discarding the supernatant, and re-dispersing in water.

Nanorattle synthesis

SERS nanorattles used as an internal standard were synthesized as described with modifications.[37] This is achieved in three major steps. **In step 1**, A silver shell was grown around the gold nanostructures (18 nm) (AuNP), which subsequently transformed into a porous gold shell using galvanic replacement reaction. To grow the silver shell on AuNP, polyvinylpyrrolidone (PVP) was employed as the stabilizing agent. Silver nitrate ($AgNO_3$) solution (5 mM) was added to the above mixture and stirred vigorously for 10s. The reaction solution was left undisturbed for 2-3 days to allow the formation of Ag@AuNP nanostructures at room temperature. The size of the silver shell was adjusted by changing the amount of precursor AuNPs seeds or by changing amount of $AgNO_3$ solution. Galvanic replacement reaction was employed to transform the silver shell on AuNP into a porous gold shell. The Ag@AuNP solution was centrifuged for 10 min at 8000 rpm and suspended in 1-mM PVP solution. The PVP-modified Ag@AuNP solution was brought to boil by heating to 100 °C. HAuCl4 (1 mM) solution was added to the Ag@AuNPs, while the solution was constantly stirred. Addition of gold salt was stopped once the solution turned a vibrant blue/purple color. **In step 2**, cage like nanorattles obtained in first step were centrifuged two times at 8000 rpm and redispersed in a mixture of 2-[7-(1,3-dihydro-1,3,3-trimethyl-2H-indol-2-ylidene)-1,3, 5-heptatrienyl]-1,3,3-trimethyl-3H-indolium iodide (HITC) (or Methylene Blue/Rose Bengal)(0.1 mM) and 1-tetradeconol(10 mg) in 200 µl of ethanol at ~100^{o}C to load the reporter molecules in interstices gaps between the cage and core. The reaction was allowed to proceed for 1 hr to evaporate most of the ethanol and dispersed in ice cold water to solidify the reporter dye inside the porous nanorattle. The solidified 1-tetradeconol at low temperature (4^{o}C) was slowly separated from nanorattles in water using 1 ml pipette. Then the nanorattle solution was centrifuged 3-5 times to completely remove the trace HITC molecules. The detailed procedure to load dyes and drugs is available in previous reports.[38-40] Finally, in step 3, to protect the reporter molecules leaking out from the nanorattles in physiologically complex condition, gold shell was grown using a seed-mediated growth method. Briefly, a gold shell on nanorattles was synthesized using 10 ml of growth solution containing 4.5 mM $HAuCl_4$ and 1 ml of 0.1-M ascorbic acid. Then 1 ml of 1-nM porous nanorattles loaded with reporter molecules were added to the above growth solution and stirred vigorously for 10 sec. The reaction mixture was let undisturbed (overnight) to form a uniform solid shell.

Oligonucleotide sequences

In this study, the Cy5-labeled stem-loop, amino-modified stem-loop and placeholder oligonucleotides are 5'-thiol-CTCTATAAGT GGTGTAGGGATTATAGAG-Cy5-3', 5'-thiol-CTCTATAAGTGGTGT AGGGATTATAGAG-NH_2-3' and 5'-GAAAGCGACTCTATAATCCCTA CACCAC-3', respectively. The synthetic DNA target and non-complementary sequences used for the demonstration are 5'-AAAGCTGAGGAGGTGGTGTAGGGATTATAGAGTCGCTTTCAAGAT AAATT-3' and 5'-TCATCCATGACAACTTTGGTATCGTGGAAGGACT CATGAC-3', respectively. All oligonucleotides were purchased from Integrated DNA Technologies, Inc (Coralville, IA).

Cy7-labeled stem-loop probe preparation for ex vivo and in vivo testing

The amino-modified stem-loop oligonucleotides were incubated with 10-times molar excess of Cy7-NHS ester dyes (Lumiprobe, FL) in 0.1 M $NaHCO_3$ solution (pH 8.5) overnight at room temperature. The free dyes were removed by desalting in NAP-5 columns (GE Healthcare).

iMS nanosensor synthesis

The stem-loop DNA probes at final concentration of 0.1 µM were incubated with 0.1 nM nanostars in 0.25 mM $MgCl_2$ solution overnight at room temperature. To stabilize the nanosensor, 1 µM of O-[2-(3-Mercaptopropionylamino)ethyl]-O'-methylpolyethylene glycol (mPEG-SH, 5000) was added to the solution for 30 min. The functionalized nanosensors were washed once with Tris-HCl buffer (10 mM, pH 8.0) containing Tween 20 (0.01%) by centrifugation at 7000 rpm for 10 min. The metallic surface of nanostars was then passivated using 0.1 mM 6-mercapto-1-hexanol (MCH) in order to displace non-specifically adsorbed probes and to prevent the probes from laying on the metal surface. The nanosensors were then washed three times with Tris-HCl buffer (10 mM, pH 8.0) containing Tween 20 (0.01%) by centrifugation at 7000 rpm for 10 min. To turn off the SERS signal, the nanosensors were incubated with 0.1 µM placeholder DNA in PBS buffer solution overnight at 37 °C. The excess placeholder molecules were removed using repeated centrifugation at 7000 rpm for 10 min. The purified nanosensors were finally resuspended in PBS.

iMS-embedded poly-NIPAM matrix synthesis

1-mL of iMS nanosensor solution was centrifuged at 7,000 rpm for 10 min. After removing the supernatant, iMS was resuspend in 1-mL PBS solution of 90 mg N-Isopropylacrylamide (NIPAM), 10 mg Acrylamide, 3 mg N,N'-Methylenebis(Acrylamide) (BIS) and 1 mg Ammonium Persulfate (APS). 2-µL N,N,N',N'-Tetramethylethylenediamine (TEMED) was then added and mixed well. 100-µL aliquots was immediately dispensed into 1.5 mL centrifuge tubes. After 1 hr, gels were removed and placed in 50 mL of PBS and allowed to soak for 12 hr to remove any unreacted monomer.

NIR Raman/SERS instrumentation

Raman spectra were recorded with a PIXIS:100BReX CCD mounted to a LS-785 spectrograph (1200 g mm^{-1} grating), controlled by LightField software, from Princeton Instruments (Trenton, NJ). A 785 nm diode laser was fiber-coupled to an InPhotonics RamanProbe (Norwood, MA) for excitation; the collection fiber of the RamanProbe was coupled to the entrance slit of the LS-785 spectrograph.

Animal studies

All animal work was conducted in compliance with the Duke University Institutional Animal Care and Use Committee and was part of a program fully accredited by the Association for the Assessment and Accreditation of Laboratory Animal Care International (Frederick, MD). Male Yorkshire pigs (15-20 kg) (Wesley Looper Pig Farm, Durham, NC) were anesthetized initially with intramuscular injection of ketamine and xylazine, then maintained on 2-4% isoflurane in O_2 to effect for the duration of the procedure. The dorsal skin was shaved then scrubbed three times with alternating chlorhexidine gluconate and 70% isopropyl alcohol. Pigs were placed prone on a heating pad and draped to create a sterile operating field. The nanosensors were intradermally injected into the superficial to mid-dermis on the dorsum of the pig.

All *ex vivo* human tissue work performed in this study received exempt approval from the Duke University Institutional Review Board. Since all specimens were de-identified within the operating room, the study protocol was determined to be exempt from full committee review. Specimens were acquired directly from the operating room once the skin had been discarded by the surgical team and was not needed by the Pathology Department. Full thickness skin specimens were maintained on moist surgical sponge at 4-23°C for less than 24 hours. Skin specimens were draped over a firm surface. The nanosensors were intradermally injected into the superficial to mid-dermis.

Results and discussion

Gold nanostar vs. silver-coated gold nanostar SERS intensity comparison

In this study, a hybrid bimetallic nanostar-based platform, silver-coated gold nanostars (AuNS@Ag), was used in order to obtain a detectable NIR SERS signal *in vivo*. A detailed characterization of the AuNS@Ag has been reported elsewhere.[10] To demonstrate the SERS effectiveness of the AuNS@Ag over AuNS, we prepared samples of each, labeled with the dye IR-780. As can be seen in Figure 2, the AuNS@Ag provide over an order of magnitude increase in SERS signal compared to the AuNS. This enhancement will be crucial to obtaining a detectable signal *in vivo*. The silver coating also blue-shifts the plasmon of the nanoparticles so that they are no longer resonant with the laser wavelength, greatly reducing photothermal transduction and the risk of heat-related injury to tissue.

iMS nanosensors for NIR-SERS detection

The iMS nanosensor performance including the detection specificity and sensitivity has been evaluated *in vitro* in PBS and reported elsewhere using a Cy5 dye as the SERS reporter.[32-34] In order to develop the iMS for *ex vivo* and *in vivo* measurements using a 785 nm diode laser, a Cy7 NIR dye-labeled iMS nanosensor was prepared in this study. Figure 3 shows the *in vitro* tests of the Cy7-labeled iMS nanosensor. In the presence of 1 µM synthetic target DNA (spectrum a), the SERS intensity was significantly increased compared to the blank sample in the absence of target DNA (spectrum b). The result indicates that the hybridization between targets and

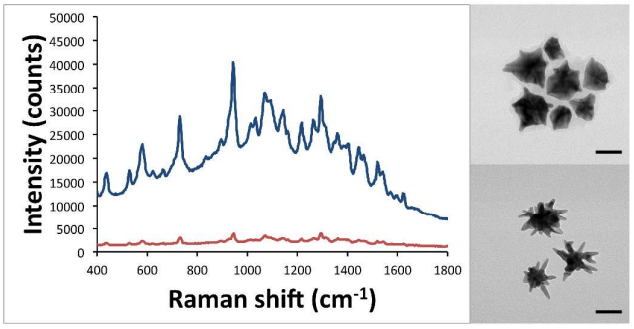

Fig. 2 SERS comparison of AuNS (red) and AuNS@Ag (blue) taken at 785 nm laser excitation (150 mW) with a 100 ms acquisition. The top right and bottom right show representative TEM images of the AuNS@Ag and AuNS, respectively. Scale bars are 50 nm.

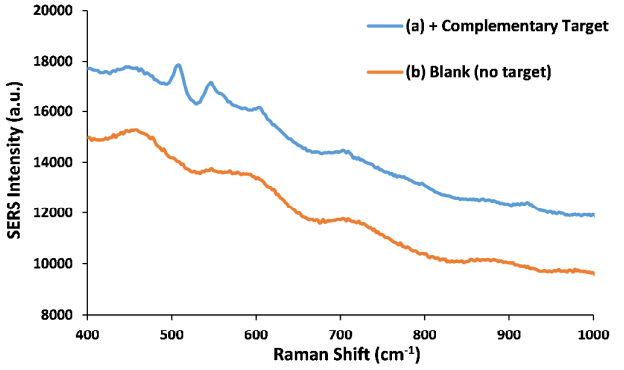

Fig. 3 SERS spectra (offset) of the Cy7-labeled iMS nanosensor in the presence (a) or absence (b - blank) of 1 µM complementary target DNA.

This journal is © The Royal Society of Chemistry 20xx

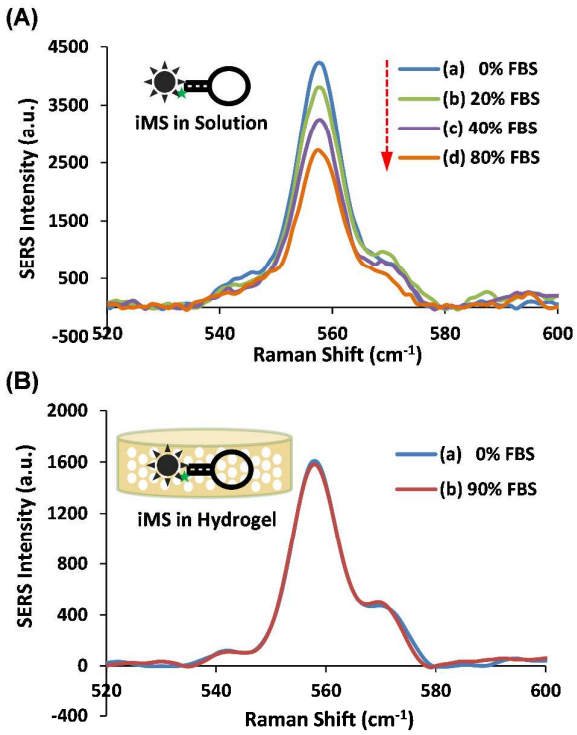

Fig. 4 (A) SERS peak signals of aqueous Cy5-labeled iMS nanosensors (0.05nM) after 1-hr incubation with 1 µM synthetic target DNA in a PBS buffer solution containing different concentrations of FBS. (a) 0%, (b) 20%, (c) 40% and (d) 80% FBS. (B) SERS peak signals of Cy5-labeled iMS nanosensors embedded in a poly-NIPAM hydrogel matrix after 3.5-hr incubation of 1 µM synthetic target DNA in a PBS buffer solution containing (a) 0% or (b) 90% FBS.

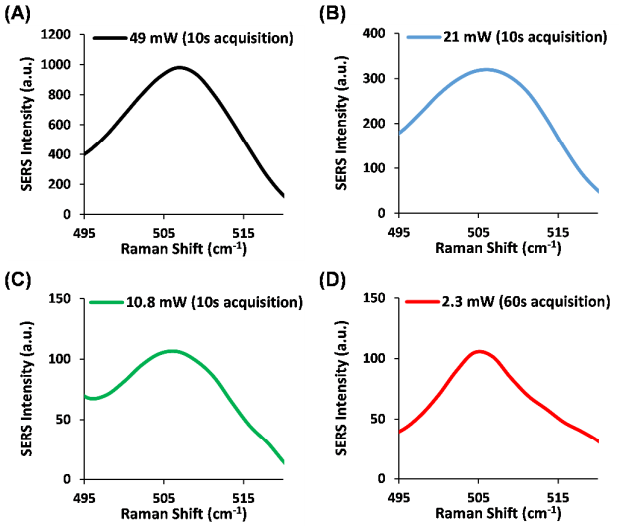

Fig. 5 NIR SERS detection of the iMS nanosensors (in the "On" status) after being injected intradermally in *ex vivo* human skin using different excitation laser powers. (A) 49 mW laser excitation with a 10-second acquisition time. (B) 21 mW laser excitation with a 10-second acquisition time. (C) 10.8 mW laser excitation with a 10-second acquisition time. (D) 2.3 mW laser excitation with a 60-second acquisition time, which is below the ANSI standard for MPE on skin at 785 nm.

placeholders enabled the formation of the stem-loop structure of the iMS, thereby moving the SERS dye onto the nanostar surface and turning the SERS signal 'On'.

Protection of iMS nanosensors from complex media in a gel matrix

In this study, we have also investigated the effect of complex media such as serum on the operation of the iMS nanosensor (Figure 4). Cy5-labeled iMS nanosensors (0.05nM) were prepared and incubated with 1 µM of synthetic target DNA in a PBS buffer solution containing different concentrations of fetal bovine serum (FBS) for 1 hour. Following incubation, SERS measurements were performed using a Renishaw InVia confocal Raman microscope equipped with a 632.8-nm HeNe laser. Figure 4A shows that increasing the concentration of FBS decreases the SERS signal of the Cy5-labeled iMS in the 'On' status. At 80% FBS (spectrum d), the SERS signal of the iMS drops to 65% of its original signal intensity (0% FBS, spectrum a), indicating that the nanosensor response was affected by the presence of FBS. To protect the nanosensor, we embedded the iMS in a poly-NIPAM gel matrix and evaluated the response of the embedded nanosensors in the complex media. Figure 4B shows that even at 90% FBS (spectrum b) the SERS signal of the iMS (in the 'On' status) is similar to that in aqueous solution (spectrum a), illustrating the excellent protection capability of a gel matrix against complex media.

***Ex vivo* NIR-SERS detection of intradermally injected iMS nanosensors through human skin**

To further examine the clinically translational capabilities of transdermal NIR SERS for in vivo monitoring, Cy7-labeled SERS nanosensors were intradermally injected in de-identified ex vivo human skin post-operationally collected at the Duke Plastic Surgery Department. The SERS signal was then acquired using a 785-nm laser. Figures 5A - C show the detected Cy7-labeled iMS SERS band at 506 cm-1 using different laser excitation power of 49 mW, 21 mW and 10.8 mW, respectively, with a 10-second acquisition time. The results also indicate that the SERS signal of the iMS could be detected in these implants even at a laser power density below the ANSI standard (Figure 5D, 2.3 mW with a 60-second acquisition time) for maximum permissible exposure (MPE) on skin at 785 nm. The spectra in Figure 5 are each averages of three acquisitions. The results demonstrated that SERS-encoded nanostars can provide an efficient platform for in vivo imaging and sensing.

Operation of iMS nanosensors using an internal standard calibration scheme for self-calibration

Please do not adjust margins

We have performed measurements to demonstrate the operation of the SERS iMS nanosensor that has an internal standard calibration scheme for sensor self-calibration. The new nanorattle SERS probe described elsewhere[37] was used as the internal standard due to core-shell nanostructure comprised of a resonance Raman reporter trapped between the core and shell. The nanorattle probe exhibits an ultra-bright SERS signal as a result of a strong and localized electric field due to plasmonic coupling at core-shell junctions. Since the SERS reporters are trapped inside the structure, they are protected by the gold shell. Like other methods such as silica-encapsulated SERS tags, the gold shell could prevent desorption of Raman reporters, making the nanorattle probe ideal for use as an internal standard. The spectrum (a) in Figure 6 shows the background-subtracted SERS signal of the nanorattle probe. It is noteworthy that the nanorattle probe and the Cy7-labeled iMS nanosensor (spectrum b) exhibit unique SERS peaks at 1288 cm^{-1} and 506 cm^{-1}, respectively. Thus, the 1288 cm^{-1} SERS peak was used to monitor the presence of internal standard while the 506 cm^{-1} SERS peak was used to monitor the operation of the iMS nanosensor.

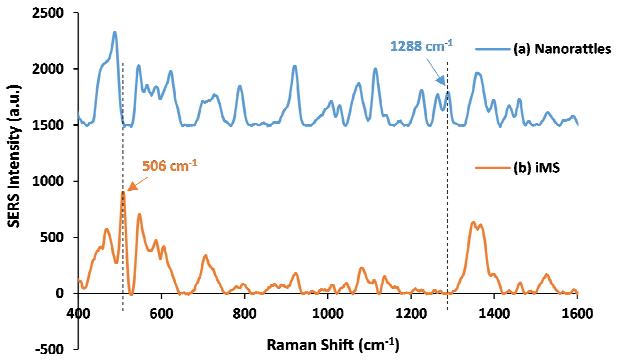

Fig. 6 Background-subtracted SERS spectra (offset) of the nanorattle probe (spectrum a) and Cy7-labeled iMS nanosensor (spectrum b). The unique SERS peaks at 1288 cm^{-1} and 506 cm^{-1} were used to monitor the presence of internal standard nanorattles and the operation of the iMS nanosensor, respectively.

Demonstration of the operation of the iMS nanosensor with the internal standard calibration scheme was performed by mixing the iMS (in the "Off" status) and the nanorattle probes. Figures 7A and 7B show the resulting SERS spectra

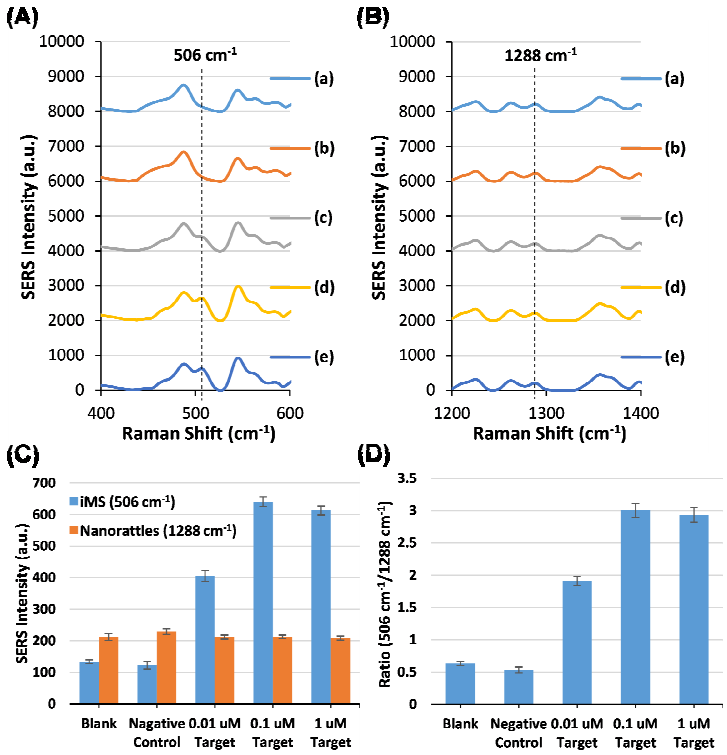

Fig. 7 *In Vitro* Detection of SERS Nanosensor Using an Internal Standard. (A) The resulting SERS spectra (offset) from the mixture of the iMS nanosensor and internal standard nanorattles at 506 cm^{-1} peak used to monitor the operation of the iMS nanosensor in the presence or absence of synthetic target DNA. (a) Blank (no target). (b) 1 μM non-complementary DNA (negative control). (c) 0.01 μM target DNA. (d) 0.1 μM target DNA. (e) 1 μM target DNA. (B) The resulting SERS spectra (offset) from the mixture at 1288 cm^{-1} peak used to monitor the internal standard in the presence or absence of synthetic target DNA. (a) Blank (no target). (b) 1 μM non-complementary DNA (negative control). (c) 0.01 μM target DNA. (d) 0.1 μM target DNA. (e) 1 μM target DNA. (C) Peak height intensities of the iMS nanosensor at 506 cm^{-1} (blue bars) and the internal standard at 1288 cm^{-1} (orange bars) in the absence or presence of increasing amounts of target DNA. (B) The intensity ratios of the two peak heights in the absence or presence of increasing amounts of target DNA.

This journal is © The Royal Society of Chemistry 20xx

Please do not adjust margins

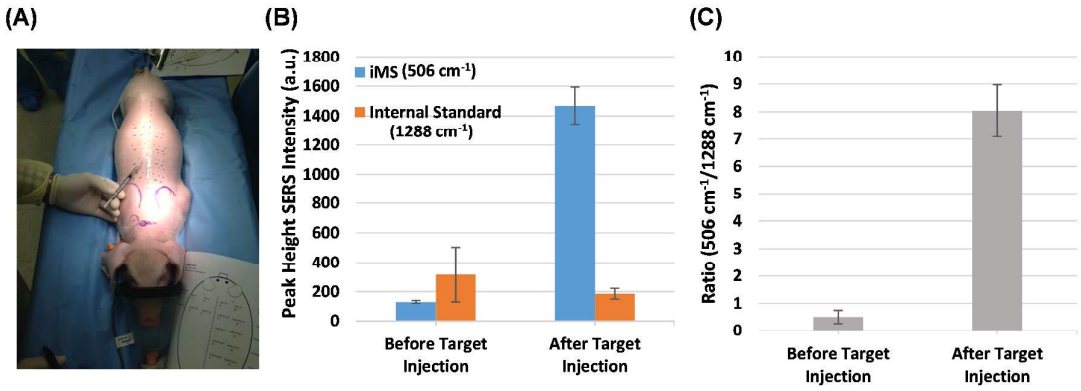

Fig. 8 *In Vivo* Measurement of SERS iMS Nanosensors in a Live Animal. (A) Photo depicts the implants after intradermal injection of nanosensors in the dorsum of a male Yorkshire pig. (B) Peak height intensities of the iMS nanosensor at 506 cm^{-1} (blue bars) and internal standard at 1288 cm^{-1} (orange bars) prior to (left) and after (right) the injection of complementary target DNA (5 nmoles). (C) The ratios of the two peak heights prior to (left) and after (right) the injection of complementary target DNA (right).

from the mixture at 506 cm^{-1} and 1288 cm^{-1}, respectively, in the presence or absence of synthetic target DNA. The experiments were carried out by adding different concentrations of complementary target (0.01 µM, 0.1 µM, and 1 µM) or 1 µM of non-complementary DNA (negative control) to the mixtures. Figure 7C shows the SERS intensity of the iMS peak height at 506 cm^{-1} and the internal standard peak height at 1288 cm^{-1}. The ratio of the two peak heights was shown in Figure 7D. The results show that while the SERS intensity of the iMS nanosensor at 506 cm^{-1} increases with increasing the amount of target DNA, the SERS signal of the nanorattle probes at 1288 cm^{-1} was not affected by addition of targets (Figure 7C). This demonstrates that the nanorattle probes can be used as the internal standard for ratio self-calibration (Figure 7D).

In vivo nucleic acid target detection using functional SERS iMS nanosensors in a live animal (pig)

After the *in vitro* evaluation, we have performed a study to investigate the performance of SERS iMS nanosensors implanted in the skin of a live pig. In this study, a mobile SERS detection system with a handheld fiber optic Raman probe was designed so that SERS nanosensor could be monitored *in vivo* by both transporting small animals to optical labs or by transporting the optical system to the animal facility for larger animals. This straight-forward setup, akin to many handheld devices currently used in doctor's offices, shows that the mobile SERS detection setup can be easily translated clinically.

For the proof-of-principle demonstration, agar gel matrices (5%) embedding iMS nanosensors mixed with internal standard nanorattles were injected intradermally into the dorsal skin of a male Yorkshire pig (Figure 8A). The agar was used as the gel matrix in this *in vivo* study to protect the nanosensors from the complex biological environment, such as blood serum, that may affect the nanosensor response. Moreover, the gel matrix also prevents diffusion of the embedded iMS nanosensors and nanorattles into body fluids. Therefore, the concentration of the embedded iMS nanosensors and nanorattles in the matrix was kept constant during the study period. This feature allows the iMS system to be used as a ratiometric nanosensor.

Following the injection of the gel matrices, 5 nmoles of synthetic target DNA were then injected and infiltrated the area surrounding the implanted matrices. The SERS signal was measured before and after the injection of target DNA using a fiber optic Raman probe placed on the skin above the implants. Figure 8B shows the peak height intensity of the iMS at 506 cm^{-1} (blue bars) and the internal standard at 1288 cm^{-1} (orange bars) prior to and after the injection of target DNA. The results show that the peak height intensity of the iMS nanosensor was significantly increased after target injection. However, a difference in the peak height intensity of the internal standard between before and after injection of the target DNA was also observed. This is due to measurement variations while repositioning the fiber optic probe on the skin above the implanted matrices after the injection of the target DNA. To minimize measurement variations, the ratio of the two peak heights (Figure 8C) was used for self-calibration. Figure 8C shows that the ratio of the two peaks was significantly increased after the injection of targets, indicating the successful use of the self-calibration scheme for the target DNA detection. The target DNA used in this study was designed to establish the proof-of-principle demonstration of a functionally working iMS nanosensor *in vivo* and its clinical relevance is beyond the scope of this study. The actual numbers of target DNA that have diffused into the gel matrices before the SERS measurements were not taken into account in this demonstration. Notes that all SERS spectra represent averages of three 10-s acquisitions using 785-nm laser excitation. The spot size of the laser is approximately 1 mm^2. This study demonstrates for the first time the feasibility of detecting nucleic acid targets using the SERS iMS nanosensor in a live animal with transdermal NIR excitation.

Please do not adjust margins

Conclusions

This study represents a proof-of-principle demonstration for *in vivo* nucleic acid target detection using a ratiometric SERS nanosensor implanted in the skin in a large animal model. Pig measurements were performed using the handheld Raman probe on live animals injected with nucleic acid targets to be monitored. In addition, *ex vivo* SERS detection of intradermally implanted nanosensors through human skin grafts using a laser power density below the ANSI standard for MPE on skin at 785 nm was also demonstrated. The results of this study illustrate the usefulness of SERS iMS nanosensors as a skin-based *in vivo* biosensing platform, laying the groundwork for a pathway to future continuous health status sensing, disease biomarker monitoring and other clinical translation applications.

Acknowledgements

This work was sponsored by the Defense Advanced Research Projects Agency (HR0011-13-2-0003). The content of the information does not necessarily reflect the position or the policy of the Government, and no official endorsement should be inferred.

Notes and references

1 A. Campion and P. Kambhampati, Chem. Soc. Rev., 1998, **27**, 241-250.
2 S. Schlücker, Angew. Chem. Int. Ed., 2014, **53**, 4756-4795.
3 T. Vo-Dinh, M. Y. K. Hiromoto, G. M. Begun and R. L. Moody, Anal. Chem., 1984, **56**, 1667-1670.
4 T. Vo-Dinh, TrAC-Trend. Anal. Chem., 1998, **17**, 557-582.
5 T. Vo-Dinh, A. M. Fales, G. D. Griffin, C. G. Khoury, Y. Liu, H. Ngo, S. J. Norton, J. K. Register, H. N. Wang and H. Yuan, Nanoscale, 2013, **5**, 10127-10140.
6 V. W. Ng, R. Berti, F. Lesage and A. Kakkar, *J. Mater. Chem. B,* 2013, **1**, 9-25.
7 H. Yuan, C. G. Khoury, H. Hwang, C. M. Wilson, G. A. Grant and T. Vo-Dinh, *Nanotechnology*, 2012, **23**, 075102.
8 H. Yuan, A. M. Fales, C. G. Khoury, J. Liu and T. Vo-Dinh, *J. Raman Spectrosc.*, 2013, **44**, 234-239.
9 F. Tian, J. Conde, C. Bao, Y. Chen, J. Curtin and D. Cui, *Biomaterials*, 2016, **106**, 87-97.
10 A. M. Fales, H. Yuan and T. Vo-Dinh, *J. Phys. Chem. C*, 2014, **118**, 3708-3715.
11 G. R. Souza, C. S. Levin, A. Hajitou, R. Pasqualini, W. Arap and J. H. Miller, *Anal. Chem.*, 2006, **78**, 6232-6237.
12 D. A. Stuart, J. M. Yuen, N. Shah, O. Lyandres, C. R. Yonzon, M.R. Glucksberg, J. T. Walsh and R. P. Van Duyne, *Anal. Chem.*, 2006, **78**, 7211-7215.
13 X. Qian, X. H. Peng, D. O. Ansari, Q. Yin-Goen, G. Z. Chen, D. M. Shin, L. Yang, A. N. Young, M. D. Wang and S. Nie, *Nature Biotechnol.*, 2008, **26**, 83-90.
14 A. Samanta, K. K. Maiti, K. S. Soh, X. Liao, M. Vendrell, U. S. Dinish, S. W. Yun, R. Bhuvaneswari, H. Kim, S. Rautela, J. Chung, M. Olivo and Y. T. Chang, *Angew. Chem. Int. Ed.*, 2011, **50**, 6089-6092.
15 K. K. Maiti, U. S. Dinish, C. Y. Fu, J. J. Lee, K. S. Soh, S. W. Yun, R. Bhuvaneswari, M. Olivo and Y. T. Chang, *Biosens. Bioelectron.*, 2010, **26**, 398-403.
16 R. McQueenie, R. Stevenson, R. Benson, N. MacRitchie, I. McInnes, P. Maffia, K. Faulds, D. Graham, J. Brewer and P. Garside, *Anal. Chem.*, 2012, **84**, 5968-5975.
17 U. S. Dinish, G. Balasundaram, Y. T. Chang and M. Olivo, *Sci. Rep.*, 2014, **4**, 4075.
18 C. L. Zavaleta, B. R. Smith, I. Walton, W. Doering, G. Davis, B. Shojaei, M. J. Natan and S. S. Gambhir, *Proc. Natl. Acad. Sci. USA*, 2009, **106**, 13511-13516.
19 M. V. Yigit, L. Zhu, M. A. Ifediba, Y. Zhang, K. Carr, A. Moore and Z. Medarova, *ACS Nano*, 2010, **5**, 1056-1066.
20 H. Kang, S. Jeong, Y. Park, J. Yim, B. H. Jun, S. Kyeong, J. K. Yang, G. Kim, S. Hong, L. P. Lee, J. H. Kim, H. Y. Lee, D. H. Jeong and Y. S. Lee, *Adv. Funct. Mater.*, 2013, **23**, 3719-3727.
21 Y. Wang, J. L. Seebald, D. P. Szeto and J. Irudayaraj, *ACS Nano*, 2010, **4**, 4039-4053.
22 A. M. Fales, H. Yuan and T. Vo-Dinh, *Langmuir*, 2011, **27**, 12186-12190.
23 J. Conde, C. Bao, D. Cui, P. V. Baptista and F. Tian, *J. Control. Release*, 2014, **183**, 87-93.
24 Y. Zhang, J. Qian, D, Wang, Y. Wang and S. He, *Angew. Chem. Int. Ed.*, 2013, **52**, 1148-1151.
25 Y. Liu, J. R. Ashton, E. J. Moding, H. Yuan, J. K. Register, A. M. Fales, J. Choi, M. J. Whitley, X. Zhao, Y. Qi, Y. Ma, G. Vaidyanathan, M. R. Zalutsky, D. G. Kirsch, C. T. Badea and T. Vo-Dinh, *Theranostics*, 2015, **5**, 946-960.
26 H. Schwarzenbach, D. S. Hoon and K. Pantel, *Nature Reviews Cancer*, 2011, **11**, 426-437.
27 P. Anker, J. Lyautey, C. Lederrey and M. Stroun, *Clinica chimica acta*, 2001, **313**, 143-146.
28 E. Gormally, E. Caboux, P. Vineis and P. Hainaut, *Mutat. Res. Rev. Mutat. Res.*, 2007, **635**, 105-117.
29 M. S. Kopreski, F. A. Benko, L. W. Kwak and C. D. Gocke, *Clinical Cancer Research*, 1999, **5**, 1961-1965.
30 P. S. Mitchell, R. K. Parkin, E. M. Kroh, B. R. Fritz, S. K. Wyman, E. L. Pogosova-Agadjanyan, A. Peterson, J. Noteboom, K. C. O'Briant, A. Allen and D. W. Lin, *Proc. Natl. Acad. Sci. USA*, 2008, **105**, 10513-10518.
31 X. Chen, Y. Ba, L. Ma, X. Cai, Y. Yin, K. Wang, J. Guo, Y. Zhang, J. Chen, X. Guo and Q. Li, *Cell Research*, 2008, **18**, 997-1006.
32 H. N. Wang, A. M. Fales and T. Vo-Dinh, *Nanomedicine: NBM*, 2015, **11**, 811-814.
33 H. T. Ngo, H. N. Wang, A. M. Fales, B. P. Nicholson, C. W. Woods and T. Vo-Dinh, *Analyst*, 2014, **139**, 5655-5659.
34 H. N. Wang, B. M. Crawford, A. M. Fales, M. L. Bowie, V. L. Seewaldt and T. Vo-Dinh, *J. Phys. Chem. C*, 2016, **120**, 21047-21055.
35 M. B. Wabuyele and T. Vo-Dinh, *Anal. Chem.*, 2005, **77**, 7810-7815.
36 H. N. Wang and T. Vo-Dinh, *Nanotechnology*, 2009, **20**, 065101.
37 N. Gandra, H. C. Hendargo, S. J. Norton, A. M. Fales, G. M. Palmer and T. Vo-Dinh, *Nanoscale*, 2016, **8**, 8486-8494.
38 L. Tian, N. Gandra and S. Singamaneni, *ACS Nano*, 2013, **7**, 4252-4260.
39 S. W. Choi, Y. Zhang and Y. Xia, *Angew. Chem. Int. Ed.*, 2010, **49**, 7904-7908.
40 G. D. Moon, S. W. Choi, X. Cai, W. Li, E. C. Cho, U. Jeong, L. V. Wang and Y. Xia, *J. Am. Chem. Soc.*, 2011, **133**, 4762-4765.

 This journal is © The Royal Society of Chemistry 20xx

Please do not adjust margins